

# DESIGN OF METHODOLOGY AND TESTS OF UTILITY PROPERTIES OF AXIAL CUTTING TOOLS

RADEK KASAN<sup>1</sup>, EMIL NECESANEK<sup>2</sup>, JOSEF SEDLAK<sup>1</sup>, STEPAN KOLOMY<sup>1</sup>, KAREL KOURIL<sup>1</sup>, LUKAS BARTL<sup>1</sup>, MARTIN MALY<sup>1</sup>

<sup>1</sup>Brno, University of Technology, Faculty of Mechanical Engineering, Institute of Manufacturing Technology, Brno, Czech Republic

<sup>2</sup>Kyjov, Nastroje CZ, s.r.o., Brno, Czech Republic

DOI: 10.17973/MMSJ.2025\_12\_2024035

[kasan@vutbr.cz](mailto:kasan@vutbr.cz)

## ABSTRACT

The aim of the experiment is to conduct drilling tests on stainless steel, process the measured data, and subsequently evaluate CZ005 drills. The drills have a different cutting-edge geometries two types of coating. For two drills, the cooling grooves on the flank were ground. Based on the evaluation, the order of the tools with the best characteristics was determined, focusing primarily on:

- accuracy of the position of individual drilled holes,
- accuracy of the diameter of the drilled holes,
- geometric tolerances of machined holes – geometric tolerance of cylindricity and perpendicularity to the drilled surface of the workpiece,
- surface texture of drilled holes – roughness,
- cutting forces,
- tool wear.

From the obtained results of the experiment, the benefits of individual coatings and ground cooling grooves were assessed. The experiment shows a procedure that can be generally applied to the evaluation of monitored parameters and the service life of drills.

## KEYWORDS

Drilling, stainless steel, TOOL wear, hole accuracy, Cutting force, Cylindricity and geometrical accuracy

## 1 INTRODUCTION

Generally material machining contains milling [1; 2], turning [3] and drilling. The drilling is often-underestimated machining method in the engineering industry. This is because many people, based on their experiences with home hobby drills, have formed a mistaken belief that it is a fully mastered and simple process. On the contrary, it is one of the most demanding machining methods from the point of view of the construction of the tool and physical influences involved. Certainly, issues such as the permanently interrupted cut during milling or the gradual change in tool geometry relative to the workpiece in turning from a larger diameter to a smaller one, bring challenges for proper chip formation which must not be overlooked [4]. However, drilling has its own specifics that are not encountered in other types of machining. From the perspective of machining technology, drilling is typically classified among the final operations within the technological process, and an inadequately managed procedure—manifested in the

destruction of the tool—entails considerable costs in the event of producing a defective workpiece.

The drilling process is a combination of two methods, namely cutting and forming, which brings difficulties in regards of tool load [5] that the tool has to deal with. The tool (drill bit) works with minimal to zero cutting speed at the point of the tip and very close surroundings. In this area, the tool does not cut, it is pressed into the material, thereby strengthening the workpiece material (see Fig. 1a) [6]. Manufacturers try to minimize this effect as much as possible by reducing the cross-section of the drill core and shortening the length of the chisel edge. However, these modifications have their limits because, as shown in the diagram of the feed force acting during machining (Fig. 1b) [7], the greatest displacement force acts precisely at the point of the tip. By greatly reducing the cross-section of the core, the tool would not withstand this force and would break. Another aspect is that cutting speed  $V_c$  increases along the entire cutting edge of the drill bit, from the center to the outer tip, reaching its maximum value, which is recommended by the tool manufacturer. At this location, there is also an accumulation of temperature, with the highest value occurring here, as shown in fig. 1c. It is the place where, due to the temperature, the greatest abrasion of the tool material occurs, in extreme cases even plastic deformation. Uneven distribution of temperature along the cutting edge can also cause stress, leading to microcracks. Finally, there is a problem with the build-up edge. This occurs at lower  $V_c$  values. As the cutting speed increases uniformly outwards, there is a high probability that it will reach a value in some area that creates conditions for built-up edge formation, which typically occurs within the range of  $V_c = 5 \div 80$  m/min [8].

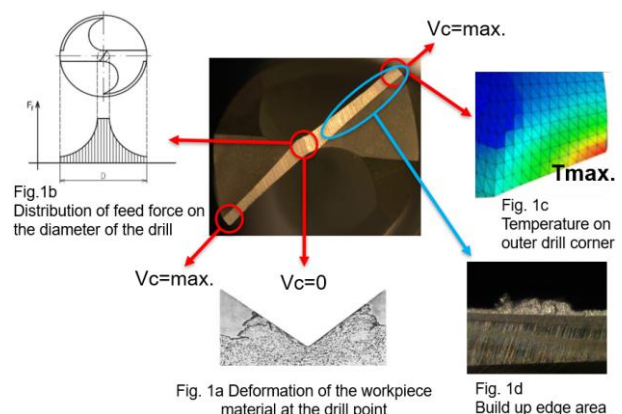


Fig. 1: Drilling process – difficulties

These facts are associated with the most common types of drill wear (as shown in Fig. 2) [9]. During the experiment, wear was observed in the form of chisel edge wear due to high pressures at  $V_c = 0$  (the forming area), and wear at the outer tip, the area with the highest  $V_c$  and temperature accumulation. Additionally, several drills showed a tendency toward built-up edge formation.

With the issue of tool wear, is closely related the term tool life. Tool life is the primary parameter for the customer in achieving dimensionally accurate and economically efficient machining of a component. Tool life is the time period from the start of the machining process until the cutting tool loses its properties and ability to cut. It is therefore evident that, in order to determine tool life, it is necessary to monitor the extent of tool wear.

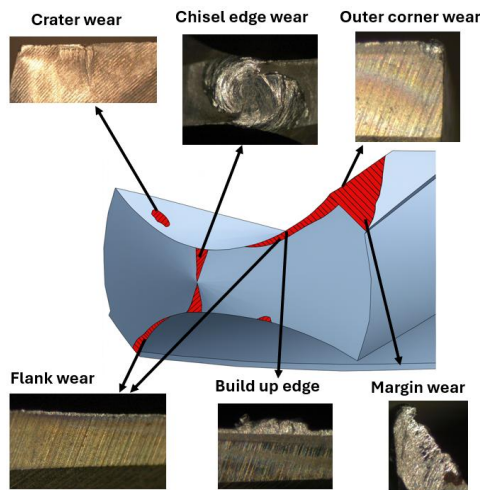


Fig. 2: Types of wear during drilling

With the issue of tool wear, is closely related the term tool life. Tool life is the primary parameter for the customer in achieving dimensionally accurate and economically efficient machining of a component. Tool life is the time period from the start of the machining process until the cutting tool loses its properties and ability to cut. It is therefore evident that, in order to determine tool life, it is necessary to monitor the extent of tool wear.

## 2 METHODOLOGY FOR DETERMINING DRILL WEAR AND TOOL LIFE

To accurately determine wear, regardless of location or the person conducting the test, it is essential to follow uniform procedures to ensure that the resulting data has consistent and comparable value. While there is a methodology that specifies recommended procedures for testing the tool life of turning tools as defined by ISO 3685 :1993 [10], and a methodology in the form of CSN ISO 8688-1(2) [11; 12] specifying tool life tests for face and end mills, no such rules have yet been established for evaluating wear and tool life in drilling. In practice, the testing of drills takes place in such a way that the procedure for determining the tool life of drills is carried out according to the imagination and invention of the persons who perform the testing.

## 3 EXPERIMENT PROCEDURE

Eleven drills with a diameter of 13.0 mm, a length of 5 x D and with different geometries were allocated for the experiment. Four uncoated drill (referred to as N), three drills with TripleCoating Cr (referred to as M) and four with Triple Coating Si (referred to as B). These are PVD coatings applied by the company SMH s.r.o. The TripleCoating Si layer is intended for machining quenched and tempered steels and difficult-to-machine materials, with or without cooling. It was expected to exhibit good resistance to elevated temperatures, which were anticipated due to the use of external cooling only. The TripleCoating Cr layer is designed specifically for machining stainless steels.

Two of the drills are equipped with a grinding modification consisting of six cooling grooves with an elliptical profile on the secondary flank. The grooves are positioned from the chisel edge toward the outer diameter of the tool to enhance the drill's cooling and lubrication performance. This region of the tool is expected to experience the highest temperature accumulation with increasing cutting speed, which must be mitigated. Drills

featuring this modification are denoted by the suffix \_CHL (see Fig. 3) [13].

For the testing, drills with different variants of cutting-edge geometries were selected. For this reason, a structured Design of Experiments (DoE) methodology was not applied for the objective evaluation of the parameters. The small number of samples did not meet the minimum replicability requirements necessary for the use of this method.

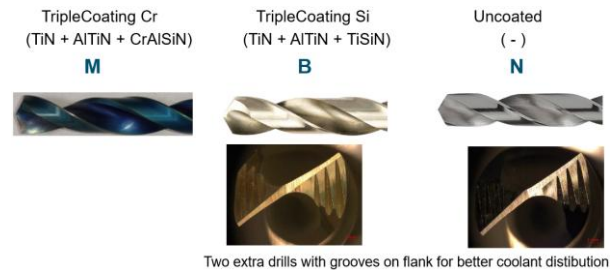


Fig. 3: Types of tested drills

The workpiece for testing was a rolled plate made of austenitic stainless steel 1.4301, X5CrNi1810, CSN 17 240. All 42 holes were drilled into the plate with each drill (see Fig. 4). Cutting forces and torques were measured on a different but identical workpiece mounted on a second dynamometer-equipped fixture located in the machine. Measurements were made each time with a new drill and subsequently after every fourteen drilled holes. Thus, each drill was measured four times during the test.

Drilling was carried out on a TAJMAC ZPS MCV 1290 machine without pre-drilling a center hole. External cooling and lubrication were provided by the Quaker Cool 7350BFF emulsion, with a concentration of 11% and a cooling pressure of 12 bar. Before drilling, the circumferential runout of each drill was checked in the machine with a maximum acceptable tolerance of 0.03 mm. Cutting parameters were the following:

$V_c = 32 \text{ m} \cdot \text{min}^{-1} \Rightarrow \text{revolutions } n = 784 \text{ rev} \cdot \text{min}^{-1}$ , feed per revolution  $f = 0.2 \text{ mm}$ .



Fig. 4: Grid of drilled holes.

Based on the dimensions shown in Figure 4, the spacing between the drilled holes might appear insufficient, as the wall thickness between adjacent holes is only 1 mm. This spacing was chosen on the basis of previous experience from similar tests conducted in austenitic stainless steel. Such a wall thickness provides adequate allowance for potential strain hardening, which typically ranges from 0.02 mm up to an extreme of 0.3 mm. The measured cylindricity values for all holes across multiple layers did not indicate any collapse or distortion of the inter-hole wall.

## 4 MEASUREMENT, MEASURING DEVICE

To evaluate the service life of the drills, the results obtained using different measurement methods were compared. In addition to measuring tool wear itself with a Zeiss optical microscope, torque and feed cutting forces were recorded using a Kistler dynamometer. Furthermore, the accuracy of the machined holes was assessed, including cylindricity, positional

deviation relative to the nominal location, deviations from the nominal diameter, and squareness to the machined surface, using a Hexagon Global S CMM. Surface roughness of the holes was measured with a Surtronic profilometer (see Fig. 5). Due to their extensive nature, the specific measurement procedures and equipment settings are not described here. All measurements were carried out in accordance with the recommendations of the equipment manufacturers and the relevant standards applicable to each measured parameter.



Fig. 5: Measurement devices

## 5 EVALUATION PROCEDURE

The original idea was to categorize drills according to the type of coating into separate groups. From each coating group (B, M, N), select the tool with the best parameters and then compare them with each other. However, this approach might eliminate tools placed in the second and following positions, which could have better parameters than the drills in the top positions within the given coating group (B, M, N). For this reason, an overall comparison was made, i.e. all drills together.

Another discussion took place on whether to combine the evaluation of cutting forces and torques with one of the evaluated categories of wear, or with the dimensional and geometric accuracy of the drilled holes. This possibility would be considered if the obvious correlation between these categories was observed. However, during the evaluation, it became clear that these influences are so individual for each tool that they cannot be applied to all. For example, with some drills wear led to an increase in the deviations of the cylindricity from the nominal value over time, with others the opposite.

Based on these considerations, the formula for the overall evaluation of drills looks like fig. 6. A view of this algorithm might suggest assigning different weights to each evaluated category. For instance, if the requirement were to emphasize drill wear itself, the ratios could be adjusted to 50% for wear assessment, 25% for the evaluation of dimensional and geometric hole properties, and 25% for the assessment based on the measured feed force and torque. However, prior to the drill testing, it was agreed with the drill manufacturer that the primary objective would be to monitor the correlations between the individual categories—specifically, whether more pronounced tool wear would manifest in deteriorated hole quality and increased forces and torques. For this reason, equal weight was assigned to all categories.

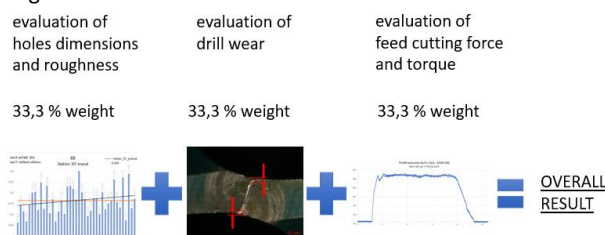


Fig. 6: Evaluation procedure

### 5.1 Evaluation of dimensional and geometric deviations of drilled holes

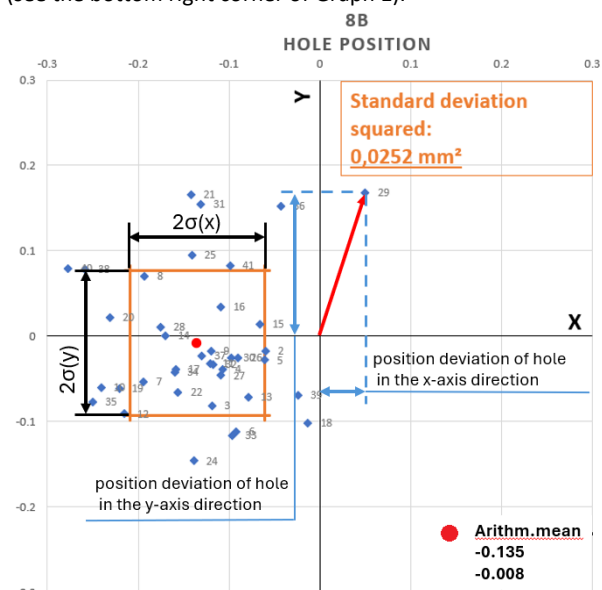
The results were obtained by a statistical analysis of data collected by measuring deviations from nominal dimensions of all 42 holes. For the correctness of the results with the minimization of distortion, several monitored parameters were always evaluated for each drill. Each evaluated parameter of the given drill was then scored from 1 for the best result to 11 for the worst. By summing the scores from all parameters, a number was obtained that determined the order of the drill in the given category, see Tab. 1. The drill with the smallest sum showed the best properties in the given category and vice versa.

- Evaluation of the position of the center the drilled holes

Graph 1 shows the distance of the calculated arithmetic mean of the center of the holes (red point) from the ideal position, represented in the graph by the intersection of the X and Y axes. The blue points are visualizations of the measured deviations of individual holes in specific axes. The graph is supplemented with a rectangle representing the standard deviation,  $\sigma$ . By calculating this range of  $\pm 1\sigma$  for both X and Y axes and plotting these values on the graph, a defined rectangle was obtained within which the majority (approximately 68%) of the holes fall. Subsequently, the area of this rectangle was calculated. A smaller rectangle area indicates that a greater number of holes were drilled closer to the arithmetic mean of the position, which signifies a more stable process.

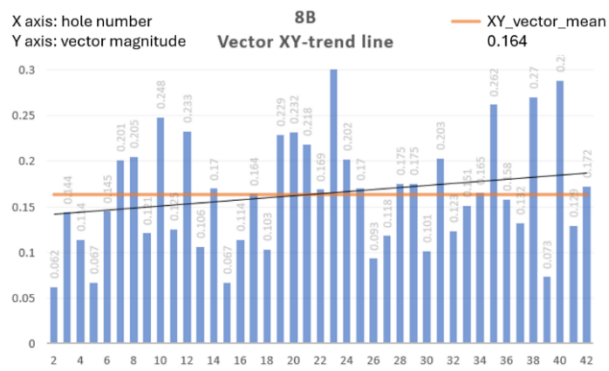
Graph 2 shows the size of the deviation vector from the XY axes, representing the actual position of the hole position from the correct position. Before plotting the values on the graph, the length of the deviation vector for each hole was calculated. Since it is the hypotenuse of a right-angled triangle, the Pythagorean theorem was used for the calculation, where the deviations represent the legs of the triangle (see Graph 1). The graph of vector size illustrates the development of deviations from the correct position over time.

The size of the area of the standard deviation rectangle and the average value of the size of the XY vector of the drills were assessed. In the case of the same sum, consideration was given to the absolute values of the arithmetic mean for each axis X and Y (see the bottom right corner of Graph 1).



Graph 1: Rectangle of the standard deviation and magnitude of the XY deviation vector





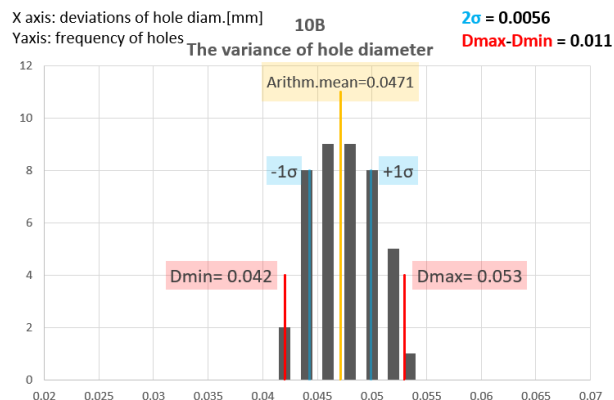
Graph 2: Magnitudes of the XY deviation vectors of the drilled holes

Drill	7B	8B	10B	21B_CHL	1M	2M	11M	15N	32N	33N	25N_CHL
Stand.deviation squared	0.0184	0.0252	0.0048	0.0074	0.0423	0.0361	0.0084	0.0127	0.0207	0.0117	0.0112
Value	7	9	1	2	11	10	3	6	8	5	4
XY vector arith.mean	0.096	0.164	0.045	0.067	0.213	0.228	0.135	0.082	0.089	0.129	0.099
Value	5	9	1	2	10	11	8	3	4	7	6
Trend line	→	→	→	→	↗	↗	→	→	→	→	→
Sum	12	18	2	4	21	21	11	9	12	12	10
Final ranking	7	9	1	2	10	11	5	3	6	8	4

Tab. 1: Parameters evaluation of the position of the centers

Table 1 presents the final evaluation in terms of the positional deviation of the hole centers from the nominal value. The value of the calculated deviation-rectangle area and the magnitude of the X\_Y vector determined the ranking within these two assessed categories. If the sum of these categories was identical, as in the case of drills 1M and 2M, the direction and magnitude of the trend-line angle were taken into account.

- Evaluation of the deviation from the diameter of the drilled holes, their cylindricity and perpendicularity. The evaluation was conducted similarly to the analysis of the hole center positions. The values of deviations from the nominal dimension, or the reference cylinder and the reference plane in the case of cylindricity and perpendicularity assessment, were plotted in graphs from which the evaluated parameters can be read. In addition, the nature of the data also allowed the creation of a normal distribution histogram (see Graph 3).



Graph 3: Histogram of hole diameter deviations

This histogram shows how many drilled holes out of the total number fell within the predefined limits of the measured deviations. The blue lines indicate the boundary  $\pm \sigma$  – the size of the standard deviation. The ideal situation would be if the graph showed only one column, i.e., the process is 100% stable, but this is never achieved in practice.

## 5.2 Evaluation of the roughness of drilled holes

The main factors influencing the surface roughness of holes during drilling include the feed rate, sufficient rigidity of the machine-tool-workpiece that minimizes vibrations, and the use of a process fluid of the correct concentration. Out of all 42 holes drilled with one drill, three holes from each row were measured, thus a total of nine. Each then once at the front part, before half and then behind half of the hole's depth. During data processing, it was found that the surface roughness of the drilled holes could fatally affect the results. An important factor influencing roughness is the tip radius. The roughness value and feed rate are related to the tip radius (in the case of drilling, this refers to the outer tip radius). With an increasing tip radius, a higher feed rate can be used without affecting the growth of roughness, or better roughness can be achieved while keeping the feed (see Fig. 7) [14].

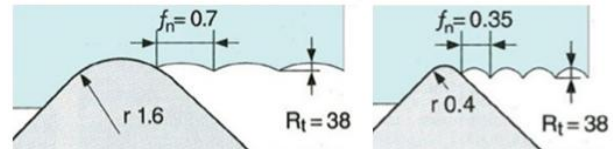
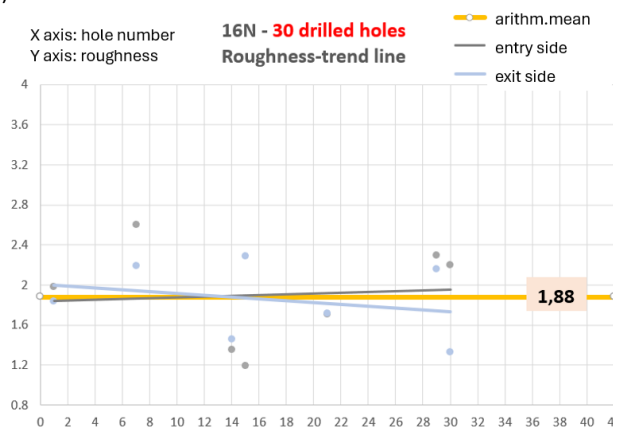


Fig. 7: The relationship between tip radius size feed size and roughness

Graphs were created from the roughness measurements showing the development trends over time for the front and rear parts of the holes separately, including the arithmetic mean (see Graph 4). The graph for drill bit 16N was deliberately chosen, as it drilled holes with lower roughness compared to the other drill. However, this tool was excluded from the test - the heavy wear of the drill did not allow the test to be completed safely (see Fig. 8).



Graph 4: Hole surface roughness - 16N drill



Fig. 8: Outer corner wear of drill 16N

The trend of improving the roughness with the increasing number of drilled holes in the tough material used for the tests is, however, related to such a negative phenomenon as the increase in wear that it cannot be considered as an indicator of good development. As there is, based on previous findings, an assumption that the evaluation of the drills is influenced by data with a poor predictive value, **the evaluation of roughness was omitted for the overall assessment of the drills.**

### 5.3 Overall evaluation of drills in terms of dimensional and geometric deviations of drilled holes

Table 2 presents the overall ranking of the drills with respect to their ability to produce holes, evaluated in terms of dimensional and geometrical characteristics — namely the positional accuracy of the drilled hole center relative to the nominal position, diameter accuracy, cylindricity, and perpendicularity to the workpiece surface. The overall ranking was determined by summing the individual ranks obtained in each evaluated category. A lower total score indicates a better position in the ranking. The table also provides a comprehensive overview of the drills' rankings in each specific category.

Drill designation	7B	8B	10B	21B_CHL	1M	2M	11M	15N	32N	33N	25N_CHL
Center position	7	9	1	2	10	11	5	3	6	8	4
Accuracy of diameters	5-6	7	2	5-6	4	8	1	9	10	11	3
Cylindricity	6	9	1	7	11	4	3	5	8	10	2
Perpendicularity	4	10	3	8	7	6	9	11	5	2	1
Sum	22-23	35	7	22-23	32	29	18	28	29	31	10
Final ranking	4-5	11	1	4-5	10	7-8	3	6	7-8	9	2

**Tab. 2:** Evaluation of dimensional and geometric tolerances of drilled holes

### 5.4 Evaluation of the feed force and torque

The data obtained by the dynamometer in the amount of 7000 records/second contained in its native form both the drill entry into the material and its exit. Given that these segments are influenced by various physical processes, whose observation and effects were not examined in this experiment, the corresponding data were filtered out (see Fig. 9).

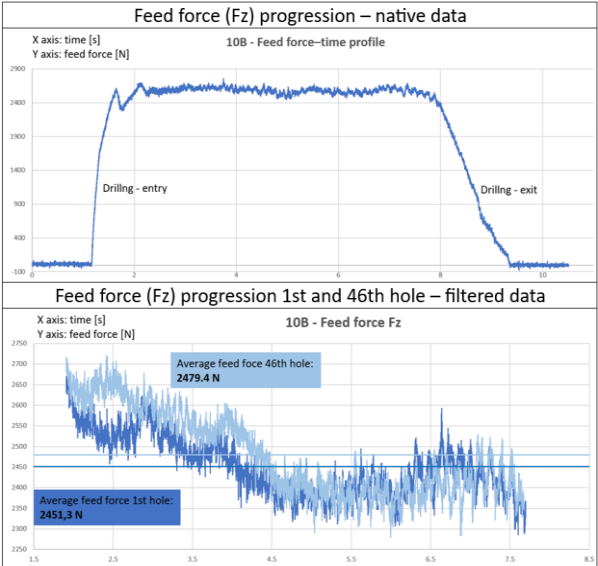
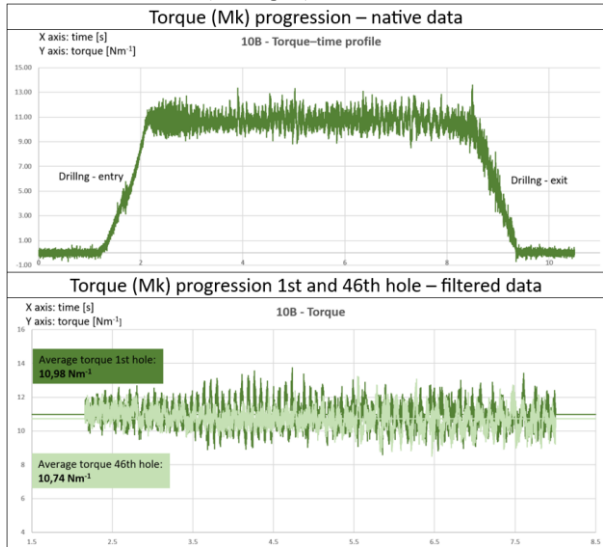
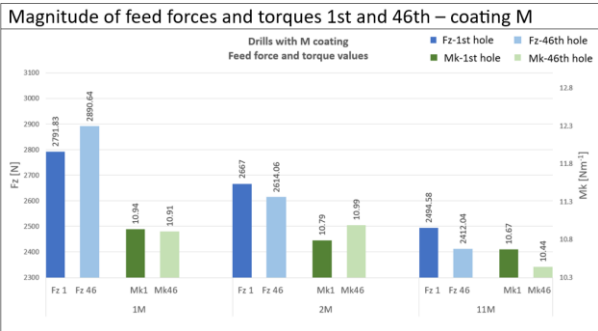


**Fig. 9:** Native and filtered data of torque and feed force

The data filtering process was simplified by the fact that the dynamometer was activated at the same moment in time for each drill, at an identical distance between the drill and the workpiece, and it recorded a time stamp for every measured value. The acquired data for all drills were processed in MS Excel. The torque and feed-force values together with the corresponding time data were plotted for the first drill, see Fig. 9. From this graph, the exact trimming times—i.e., the end of tool entry and the beginning of tool exit—were determined. These boundary time values were subsequently applied to all drills in such a way that all torque and feed-force values recorded prior to the entry time and after the onset of the exit phase were removed. These filtered values were used to calculate the average value for individual feed forces, size and moments for both the first and last hole. The values were plotted into bar graphs (see Graph 5), from which it was possible to read the difference in torque values of both the 1st and 42nd holes of individual drills, as well as all drills with each other. The data indicate that the torque values are small enough to be considered equal. Therefore, the overall evaluation of the drills will be assessed only on the basis of feed force. The value of the torque will only be considered when the results if there are equal results in the feed forces.



**Graph 5:** Values of feed forces size and torques

### 5.5 Overall evaluation of drills based on feed force

To evaluate the drills in terms of thrust force, the arithmetic mean of the thrust force measured on the first and the last hole was calculated for each individual drill. These arithmetic mean values directly determine the ranking of the drills in this category. The drill with the lowest mean thrust force is ranked

1st, while the drill with the highest mean thrust force is ranked 11th (see Table 3).

	Units	7B	8B	10B	21B_CHL	1M	2M	11M	15N	32N	33N	25N_CHL
Mean value of feed force Fz [N]		2735	2769	2465	2579	2841	2641	2453	2530	2992	2715	2508
Final ranking		8	9	2	5	10	6	1	4	11	7	3

Tab. 3: Evaluation of drills in terms of feed force

### 5.6 Overall Evaluation of drill wear

On the basis of enlarged photos and direct measurements on a microscope, the most critical areas regarding drill wear were evaluated:

- Tip wear - as this applies to both sides of the tip, the arithmetic mean of these wears was used for the output, see Fig. 10.
- Flank wear – flank wear of the drill bit appeared in all samples only around the tip. This type of wear was not observed in any of the samples elsewhere on the primary flank surface. The order of the drills was subsequently determined directly from the magnitude of this wear in a given area (see Table 4).

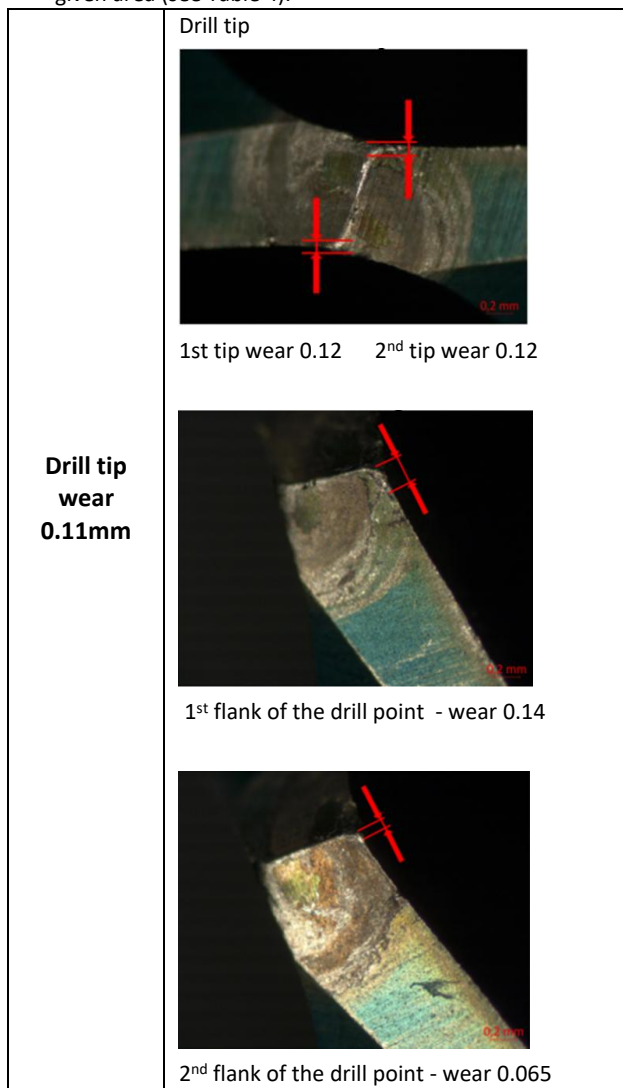
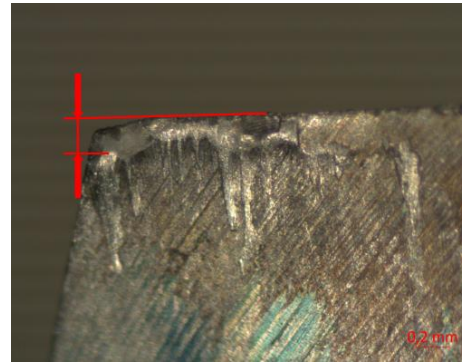


Fig. 10: Measurement of drill tip wear

- Outer corner wear – this wear was measured both along the edge line of the drill and perpendicular to it (see Fig. 11). Wear measurement was naturally carried out on both outer corners of the drill. The order was again determined by the wear value.

### Axial outer corner wear



### Radial outer corner wear

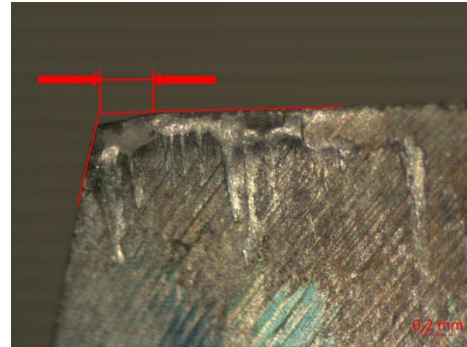


Fig. 11: Measurement of outer corner wear – two directions

- Propensity to the build-up edge - the overall occurrence build-up edge at the outer tip and along the entire length of the edge was assessed. Three levels of buildup were established: none, slight, and greater.

The data of all observed types of wear were recorded in a table. Based on the arithmetic mean values of wear on both cutting edges of the drill, the order of the drills in individual wear categories was determined (see Table 4). The total evaluation was obtained by the sum of these rankings. The drill bit with the lowest total score exhibited the least wear and vice versa.

Wear	Drill	P	7B	P	8B	P	10B	P	12B	P	21B_CHL
Tip		6	0.08	3	0.062	8	0.1	7	0.088	1	0.025
Tip – near area											
1. Flank	4	0.04	6	0.09	4	0.04	6	0.08	2	0.01	
2. Flank	3	0.026	3	0.026	7	0.044	1	0	2	0.01	
1. Face	5	0.026	1	0	2	0.01	7	0.1	3	0.02	
2. Face	6	0.03	8	0.133	2	0.01	1	0	1	0	
Sum	18		18		15		15		8		
Order	6		6		5		5		3		
Outer corner											
1. A) Face	3	0.035	2	0.026	3	0.035	2	0.026	2	0.026	
1. B) Face	4	0.035	7	0.08	3	0.018	7	0.08	5	0.06	
2. A) Face	9	0.16	8	0.14	5	0.08	3	0.035	2	0.03	
2. B) Face	5	0.04	8	0.11	6	0.09	4	0.018	7	0.1	
3. Sec flank	1	0	1	0	1	0	1	0	1	0	
4. Sec flank	1	0	1	0	1	0	1	0	1	0	
Sum	23		27		19		18		18		
Order	6		7		4		3		3		
Build-up edge	0	none	0	none	0.5	slight	0	none	0	none	
Total sum	18		16		17.5		15		7		
Final ranking	7		5		6		4		2		

Wear	Drill	P	1M	P	2M	P	11M	P	15N	P	32N	P	33N	P	25N_CHL
Tip		9	0.11	10	0.12	5	0.075	6	0.08	8	0.1	2	0.05	2	0.05
Tip – near area															
1. Flank	3	0.035	8	0.13	1	0	2	0.01	5	0.044	2	0.01	1	0	
2. Flank	4	0.03	8	0.13	1	0	2	0.01	6	0.04	5	0.035	2	0.01	
1. Face	1	0	8	0.13	1	0	1	0	4	0.022	6	0.044	1	0	
2. Face	5	0.026	9	0.14	3	0.17	3	0.017	4	0.022	7	0.08	1	0	
Sum	13		33		6		8		20		20		5		
Order	4		8		2		3		7		7		1		
Outer corner															
1. A) Face	2	0.026	6	0.07	1	0.017	5	0.06	4	0.044	7	0.24	1	0.017	
1. B) Face	4	0.035	6	0.07	2	0.012	8	0.09	8	0.09	9	0.2	1	0.01	
2. A) Face	4	0.06	10	0.19	4	0.06	6	0.09	7	0.11	6	0.09	1	0.026	
2. B) Face	8	0.11	3	0.022	7	0.1	6	0.09	9	0.2	2	0.02	1	0.01	
3. Sec flank	1	0	1	0	1	0	2	0.02	1	0	3	0.04	1	0	
4. Sec flank	2	0.02	1	0	1	0	1	0	1	0	1	0	1	0	
Sum	21		27		16		28		30		28		6		
Order	5		7		2		8		9		8		1		
Build-up edge	0	none	0.5	slight	0.5	slight	1	bigger	1	bigger	1	bigger	0	none	
Total sum	18		25.5		9.5		18		25		18		4		
Final ranking	7		9		3		7		8		7		1		

Tab. 4: Evaluation of drills wear

## 6 FINAL EVALUATION OF DRILLS

The final evaluation of the drills is based on the sum of ranks from all previous criteria (see Table 5):

- the ranking of drills according to dimensional and geometrical deviations of the drilled holes from nominal values,
- the ranking based on cutting torque and thrust force magnitude,
- the ranking based on measured tool wear.

By simply adding up the ranks from all categories, the overall final ranking was obtained. From this ranking, three drills clearly stand out with excellent performance.

Drill designation	7B	8B	10B	21B_CHL	1M	2M	11M	15N	32N	33N	25N_CHL
Evaluation of dimensional and geometric deviations	4-5	11	1	4-5	10	7-8	3	6	7-8	9	2
Evaluation in terms of feed force	8	9	2	5	10	6	1	4	11	7	3
Evaluation of drill wear	6	4	5	2	6	8	3	6	7	6	1
Sum	18/19	24	8	11/12	26	21/22	7	16	25/26	22	6
Final ranking	6	9	3	4	11	7	2	5	10	8	1

Tab. 5: Final ranking of drills

## 7 CONCLUSION

The objective of the experiment was to conduct drilling tests whose output would enable the evaluation of eleven drills featuring different cutting-edge geometries, two types of coatings, and an uncoated variant. For two of the drills, cooling-groove grinding on the flank was performed to assess the effectiveness of this modification on tool life. The experimental results clearly demonstrate the effect of coolant distribution directly into the cutting zone for the uncoated drill 25\_N\_CHL, which emerged as the best-performing tool and exhibited very high wear resistance (see Tab. 5). It was therefore decided that drills 10B and 11M would be equipped with the same groove geometry on the flank as the 25N\_CHL drill. Drill 25N\_CHL will

additionally be coated with the M coating, and the experiment will be repeated with these three tools.

Another aim of the experiment was to establish a scoring-based evaluation procedure. Unfortunately, the approach was limited by the small sample size within each type of tested drill. In a subsequent experiment, it would be advisable to focus more closely on the weighting of the individual evaluation categories. Determining appropriate weights requires a clear understanding of which of the compared categories is of primary importance and which are secondary. The results and conclusions can be significantly influenced by such, to some extent subjective, weight assignment. From the previous evaluation, in which all categories were weighted equally, it follows that the coating exerts a strong influence on the overall ranking of the drills. When the weighting ratios are modified so that the primary emphasis is placed on wear (54%), while torque/feed-force assessment and hole accuracy each receive a weight of 23%, the evaluation changes: the drill 21B\_CHL shifts to third place. In this scenario, the conclusion would be that the cooling-groove modification has a greater impact on the drill's performance in the assessed categories.

It is evident that a scoring-based evaluation system, combined with meaningful and purposeful weighting of priorities, can provide valuable support to tool manufacturers. For example, it can more clearly indicate whether a modified design element or other tool adjustment is correct and meets expectations, or whether additional variants should be investigated when the expected performance is not achieved.

## ACKNOWLEDGMENTS

This research study was supported by the grant “Comprehensive technology for interdisciplinary work with advanced materials, emphasising their multidisciplinary applications”, FSI-S-25-8787.

## REFERENCES

- [1] S. Kolomy, M. Slany, M. Doubrava, J. Sedlak, J. Zouhar, L. Rehorek, Comparative analysis of machinability and microstructure in LPBF and conventionally processed M300 maraging steel, Scientific Reports. 15 (2025). <https://doi.org/10.1038/s41598-025-19719-8>.
- [2] S. Kolomy, M. Maly, J. Sedlak, J. Zouhar, M. Slany, P. Hrabec, K. Kouril, Machinability of extruded H13 tool steel: Effect of cutting parameters on cutting forces, surface roughness, microstructure, and residual stresses: Effect of cutting parameters on cutting forces, surface roughness, microstructure, and residual stresses, Alexandria Engineering Journal. 99 (2024) 394-407. <https://doi.org/10.1016/j.aej.2024.05.018>.
- [3] M. Drbal, S. Kolomy, J. Sedlak, J. Zouhar, J. Vitek, Investigation of the Tool Wear Progression in Parting Technology, Manufacturing Technology. 24 (2024) 901-913. <https://doi.org/10.21062/mft.2024.093>.
- [4] A. Kenfack, L. Langenhorst, J. Solter, A. Fischer, B. Karpuschewski, NUMERICAL INVESTIGATION OF TOOL WEAR EFFECTS ON PROCESS QUANTITIES DURING TURNING OF AISI 4140, Mm Science Journal. 2025 (2025). [https://doi.org/10.17973/mmsj.2025\\_11\\_2025144](https://doi.org/10.17973/mmsj.2025_11_2025144).
- [5] A. Wächter, M. von Elling, I. Uzunov, L.T. Bui, W. Haidary, M. Weigold, STUDY ON THE LOAD PROFILE CHARACTERISTICS OF MACHINE TOOLS IN MACHINING



OPERATIONS, Mm Science Journal. 2025 (2025).  
[https://doi.org/10.17973/mmsj.2025\\_11\\_2025145](https://doi.org/10.17973/mmsj.2025_11_2025145).

- [6] G.T. Smith, Cutting tool technology: industrial handbook, Springer, London, 2008. <https://doi.org/10.1007/978-1-84800-205-0>.
- [7] D.A. Stephenson, J.S. Agapiou, Metal cutting theory and practice, Third edition, Taylor & Francis Group, CRC Press, 2016.
- [8] T.N. Ivanova, P. Bozek, A.I. Korshunov, V.P. Koretskiy, CONTROL OF THE TECHNOLOGICAL PROCESS OF DRILLING, Mm Science Journal. 2020 (2020) 4035-4039. [https://doi.org/10.17973/mmsj.2020\\_10\\_2020052](https://doi.org/10.17973/mmsj.2020_10_2020052).
- [9] M.-jae Jeong, S.-woo Lee, W.-ki Jang, H.-jin Kim, Y.-ho Seo, B.-hee Kim, Prediction of Drill Bit Breakage Using an Infrared Sensor, Sensors (Basel, Switzerland). 21 (2021) 2808. <https://doi.org/10.3390/s21082808>.
- [10] ISO 3685:1993 (SVK), Skusanie trvanlivosti sustruznickych nástrojov s jednou reznou hranou, (1999).
- [11] CSN ISO 8688-1, Rezne nástroje. Testování trvanlivosti při frezování. Cast 1: Rovinné frezování, Rovinné Frezování. (1993).
- [12] CSN ISO 8688-2, Rezne nástroje. Zkoušení trvanlivosti při frezování, Celní Frezování. (1993).
- [13] J. Sedlak, J. Zouhar, S. Kolomy, M. Slany, E. Necesánek, Effect of high-speed steel screw drill geometry on cutting performance when machining austenitic stainless steel, Scientific Reports. 13 (2023) 9233-9233. <https://doi.org/10.1038/s41598-023-36448-y>.
- [14] M. Stulpa, Technologie obrábění: cnc soustružení, frezování, vrtání : pro praxi, Grada publishing, Praha, 2022.

MSc. Stepan KOLOMY, Ph.D.

Brno University of Technology, Faculty of Mechanical Engineering  
Institute of Manufacturing Technology, Department of Machining Technology  
Technická 2896/2, 616 69 Brno, Czech Republic,  
+420 541 142 408, [kolomy@fme.vutbr.cz](mailto:kolomy@fme.vutbr.cz),  
<https://www.vut.cz/en/people/stepan-kolomy-191433>

Assoc. Prof. Karel KOURIL, Ph.D., MSc.

Brno University of Technology, Faculty of Mechanical Engineering  
Institute of Manufacturing Technology, Department of Machining Technology  
Technická 2896/2, 616 69 Brno, Czech Republic,  
+420 541 142 420, [kouril.k@fme.vutbr.cz](mailto:kouril.k@fme.vutbr.cz),  
<http://www.fme.vutbr.cz/prdetail.html?pid=58840>

MSc. Lukas BARTL

Brno University of Technology, Faculty of Mechanical Engineering  
Institute of Manufacturing Technology, Department of Machining Technology  
Technická 2896/2, 616 69 Brno, Czech Republic,  
[bartl@vutbr.cz](mailto:bartl@vutbr.cz),  
<https://www.vut.cz/lide/lukas-bartl-151836>

MSc. Martin MALY

Brno University of Technology, Faculty of Mechanical Engineering  
Institute of Manufacturing Technology, Department of Machining Technology  
Technická 2896/2, 616 69 Brno, Czech Republic,  
[maly@vutbr.cz](mailto:maly@vutbr.cz),  
<https://www.vut.cz/lide/martin-maly-182781>

## CONTACTS

MSc. Radek KASAN

Brno University of Technology, Faculty of Mechanical Engineering  
Institute of Manufacturing Technology, Department of Machining Technology  
Technická 2896/2, 616 69 Brno, Czech Republic,  
[kasan@vutbr.cz](mailto:kasan@vutbr.cz),  
<https://www.vut.cz/lide/radek-kasan-12962>

MSc. Emil NECESANEK

Ltd. NASRTOJE CZ s.r.o  
Riegrova 399/2, 697 01 Kyjov, Czech Republic,  
[necesanek@nastrojecz.cz](mailto:necesanek@nastrojecz.cz)

Prof. Josef SEDLAK, Ph.D., MSc.

Brno University of Technology, Faculty of Mechanical Engineering  
Institute of Manufacturing Technology, Department of Machining Technology  
Technická 2896/2, 616 69 Brno, Czech Republic,  
+420 541 142 408, [sedlak@fme.vutbr.cz](mailto:sedlak@fme.vutbr.cz),  
<http://www.fme.vutbr.cz/prdetail.html?pid=16690>